X-band RF Transverse deflectors for the LCLS-II

LCLSII-TN-15-42

9/9/2015

Y. Ding, P. Emma, H. Loos,
Y. Nosochkov, J. Wang
SLAC, Stanford, CA 94036 USA

X-band RF transverse deflectors for the LCLS-II

Y. Ding, P. Emma, H. Loos, Y. Nosochkov, J. Wang

SLAC National Accelerator Laboratory

(9/9/2015)

Abstract

An X-band transverse deflector (XTCAV) has been successfully developed for femtosecond electron and x-ray pulse temporal diagnostic at the LCLS. With the planned LCLS-II where two undulator beamlines will be built, we discuss in this note the possible layout of the XTCAV system for the LCLS-II with sharing one Klystron station. The resolution could still achieve around 1 fs rms at 4 GeV with the help of adding SLED cavity.

1. Introduction

Transverse deflecting structures are routinely used in accelerators for bunch length and beam longitudinal phase space diagnostics. One detailed description could be found in [1]. The high frequency time variation of the deflecting fields is used to streak the electron bunch where the resulting transverse beam width measured on a simple profile monitor represents the absolute bunch length. The invention of deflecting structure is nearly 50 years old, and the first one was built at SLAC working at S-band RF frequency [2]. Higher frequency (e.g., at X-band) transverse deflectors have the potential to further improve the resolution. Based on the X-band technology developed at SLAC in the past years [3], an X-band RF transverse cavity (we called it "XTCAV") was proposed at the LCLS for lasing characterization [4, 5], and now it has been developed as an online electron and x-ray pulse temporal diagnostic at the LCLS with high resolution [6].

In the following sections, we will first discuss the existing XTCAV design and resolution at the LCLS, then discuss the proposed configuration for LCLS-II including the rf layout, optics design and stay-clear considerations.

2. The existing XTCAV at the LCLS

The existing XTCAV at the LCLS is located downstream of the undulator beamline, just before the dump dipoles. Two 1-m-long X-band RF horizontal deflecting structures are powered by one SLAC-made XL4 klystron. Some major parameters of the existing XTCAV at the LCLS are summarized in Table 1.

The high power from the klystron is transported through ~150-foot-long waveguide to the structure and equally split into the two 1-m-long structures. A phase shifter has been used for relative phase adjustment between the two structures. The electron bunch is deflected

horizontally at a zero-crossing phase in the deflector, and then vertically bent in the dump bending magnets. A downstream on-axis YAG screen (called OTRDMP in the MAD deck) is used to measure the transverse image which represents the electron bunch longitudinal phase space.

Table 1: Major parameter of the existing LCLS XTCAV (before SLED upgrade)

Parameter	Value	Unit
High power RF system		
RF frequency	11.424	GHz
XL4 klystron output power	50	MW
Total power before the structures	35	MW
Measured phase jitter rms	0.15	Deg-X
Measured amplitude jitter rms	< 0.1%	
Deflecting Structure		
RF frequency	11.424	GHz
Structure type	2π/3 backward wave	
Structure orientation	Horizontal deflection	
Effective structure length	1	m
Total flange-flange length	118.8	cm
Number of structures	2	
Number of regular cells per structure	113	
Aperture 2a	10	mm
Nominal transverse kick (on crest) @35MW *	45	MeV/c

*: The relation between the input peak rf power and the maximum kick (in MV) for **each** 1-m structure is: $kick[MV] = 5.46\sqrt{P_{in}[MW]}$ (note we have two 1-m structures with each input power 35/2 MW, and the kick strength from each structure is 45/2 MV).

We briefly discuss the resolution considerations which are related to optics design. Assuming an rf phase near zero-crossing, and the streaked horizontal beam size σ_x is much larger than the nominal beam size σ_{x0} (*i.e.*, in the absence of a deflecting voltage) on the screen, we can write the Calibration factor (also called Shear function) as:

$$S = \frac{\sigma_x}{\sigma_z} = \frac{k_{rf}\sqrt{\beta_d \beta_s}\left|eV_0 \sin \Delta\psi\right|}{E_e}. \quad (1)$$

Where σ_z is the bunch length we want to measure, $k_{rf} = \frac{2\pi}{\lambda_{rf}}$ with $\lambda_{rf} = 2.63\,cm$ for X-band rf structure, β_d and β_s are the horizontal beta functions at the deflecting location and the dump screen, V_0 is the effective deflecting voltage, $\Delta\psi$ is the horizontal phase advance between the deflecting location and the dump screen, and E_e is the electron beam energy. With this

calibration factor, we can further define the temporal resolution (with assuming beam horizontal emittance $\varepsilon_{N,x}$):

$$\sigma_{t,R} = \frac{\sigma_{x0}}{S} = \sqrt{\frac{\varepsilon_{N,x}}{\gamma\beta_d}} \frac{E_e}{k_{rf}\left|eV_0 \sin\Delta\psi\right|}. \quad (2)$$

Clearly, to get a better temporal resolution, higher RF frequency and deflecting voltage, lower e-beam emittance and energy are preferred. In addition, the optics setup should be also optimized to have a larger beta function at the deflecting cavity, and a correct phase advance $\Delta\psi$ (close to 90 deg) between the deflecting cavity and the screen.

At the vertical plane, the dump spectrometer gives the energy resolution of the electron beam:

$$\sigma_{\delta,R} = \frac{\sqrt{\beta_y \varepsilon_{N,y}}}{D_y}, \quad (3)$$

where β_y and D_y are the vertical beta function and dispersion on the screen, and $\varepsilon_{N,y}$ is the vertical emittance. Note that the transverse deflecting structure itself also induces additional energy spread on the e-beam.

With a full deflecting voltage of 45 MV at the LCLS, the measured time resolution is about 1 fs rms at 4 GeV, and about 4 fs rms at 14 GeV [6].

3. Configuration of the XTCAV for the LCLS-II

For the LCLS-II, there will be two undulator lines for SXR and HXR FELs, with high beam rate up to 1MHz from the superconducting linac. Based on the existing XTCAV rf system, an upgrade with a new SLED technology will be applied in the fall of 2015 to the LCLS XTCAV [7]. The final power will be increased by a factor 4. With this upgrade, we have the capability to power both XTCAVs at the soft and hard x-ray beamline at the LCLS-II. In the following we discuss the rf configuration, the optics design and stay clear considerations for the LCLS-II XTCAVs.

3.1 RF configuration of the XTCAV with SLED mode

To accommodate to the SLED operation, modifications of some existing RF parts have been planned in the summer of 2015 at the LCLS. The old klystron will be replaced by a new one with peak power of 50 MW, and the old modulator will be upgraded capable to deliver up to 1.5 μs high voltage pulses to the klystron in order to support the SLED mode. The new SLED cavity [7] is to be located near the klystron output window in the building 921. There will be two working modes: non-SLED mode with peak RF power 0 - 50 MW and SLEDed mode with 0-200 MW peak RF power. This high RF power is transported to the structure via a ~150-foot long

waveguide. Based on some early measurements, we assume a conservative power transmission efficiency of 70%, so the total power with SLED mode near the deflecting structure input would be about 140 MW. The high-power processing and SLED commissioning will be performed at LCLS in 2015 fall.

For LCLS-II with two beamlines, a newly designed compact power slitter [8] would be adopted. It would locate in the tunnel before the deflecting structures. The extremely flexible power splitting is realized by remotely tuning of a plunger inside a circular waveguide (see Appendix-A). The port I could deliver continuously adjustable peak power (P1 = 0 -140 MW) to the LCLS HXR line. The port 2 could deliver the other part of the power (P2 = 140 MW - P1) to the LCLS II SXR line. The splitting ratio of total power will be decided by the resolution requirements of the experimental physics. Because the power splitting has an impact to the RF phase, therefore the phase shifter in the existing LCLS deflector assembly will be removed and installed downstream of one of the power splitter output ports in order to allow both HXR and SXR lines working correctly as shown in the Figure 1. All the working status can be digitally recorded and easily recalled automatically.

The existing two 1-m-long structures will stay at the HXR beam line. The correct phase relation between two deflectors can be obtained by carefully adjusting the structure locations and minor deformation of feeding waveguides, therefore, the existing high power phase shifter (see Appendix-B) can be removed for correctly phasing the new SXR line. Two new 1-m-long structures same as the existing ones will be needed at the SXR beamline. We will keep the same electrical design, only a minor upgrade of the coupler deign to a so-called "fat lip" coupler design will be adopted for a better RF performance [9]. The deflecting is in horizontal plane as conventional like the existing ones at the LCLS.

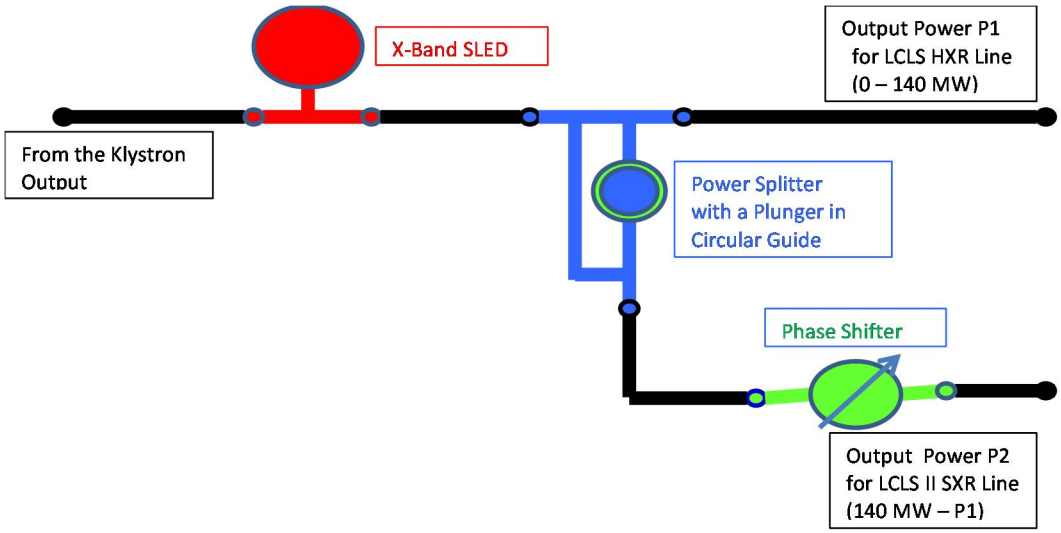

Figure 1: A schematic layout of the XTCAV RF system showing the key components: SLED assembly, Power splitter assembly and Phase shifter.

3.2 Optics design and resolution

As discussed earlier, with a fixed rf system, we should optimize the beam optics for achieving the best resolution. In general, we expect the horizontal phase advance between the deflecting structure and the imaging screen to be about 90 degrees, horizontal beta function at the deflecting structure location to be large, and vertical beta function on the screen to be small (for best energy resolution). Based on Eq. (2), the horizontal beta function at the screen does not affect the final resolution, but that is an ideal case with assuming the camera and screen have unlimited resolution. At the existing LCLS dump, we used a 1.5-inch wide YAG screen with 50 μm thickness, and the resolution is estimated to be about 30 μm. The camera is typically set with a wide region of interest to capture most of the shots jittering around the screen, and the pixel size is about 30 μm.

We list the major related Twiss parameters in Table 2 after optics optimization. The limited distance between the end of the undulator and the XTCAV prevents us from further increasing the horizontal beta function at the XTCAV location for the HXR beamline. With assuming an emittance of 1 μm, we summarize the achievable resolution for the two beamlines with a power splitting ratio 1:3. If we choose to deliver the full power to one of the beamlines, the maximum achievable resolutions are listed in the brackets with blue color, which are 0.7 fs rms for SXR beamline, and 1.7 fs rms for HXR beamline.

Table 2: The optics design and XTCAV resolution for LCLS-II.

	SXR line (4GeV)	HXR line (14 GeV)
Beta-x at XTCAV (m)	118	56
Phase advance between XTCAV and screen (deg)	70	82
Beta-x at screen (m)	22	46
Beta-y at screen (m)	1.27	5
Dispersion at screen (m)	0.46	0.46
XTCAV input power (MW): P = 35 MW	P (4P)	3P (4P)
XTCAV voltage (MV)	45 (90)	78 (90)
Time resolution rms (fs)	1.4 (0.7)	2.0 (1.7)
Energy resolution rms (keV)	110 (261*)	411 (910*)

*: Assuming the screen resolution is 30 μm, the energy resolution is determined by the screen resolution in the brackets, not the beta-y at screen.

3.3 Stay clear operation

One different feature of the XTCAV system for LCLS-II is that the screen will be set off-axis capturing only the deflected beam at 120 Hz, while the high-repetition-rate non-deflected beam will be still transported on axis to the dump. So the XTCAV will be operated slightly off the zero-crossing phase to provide a net horizontal kick. This adds complexity of the downstream

stay-clear requirement. A detailed discussion of the beam stay-clear consideration can be found in [10]. The required screen edge is about 6 mm off axis and the deflected beam trajectory centroid is about 18.5 mm at *OTRDMP*, with assuming the horizontal extent of the streaked beam about 12.5 mm full width at *OTRDMP*. In principle, we can use a YAG screen with a hole in the middle so either side of the zero-crossing phases can be used.

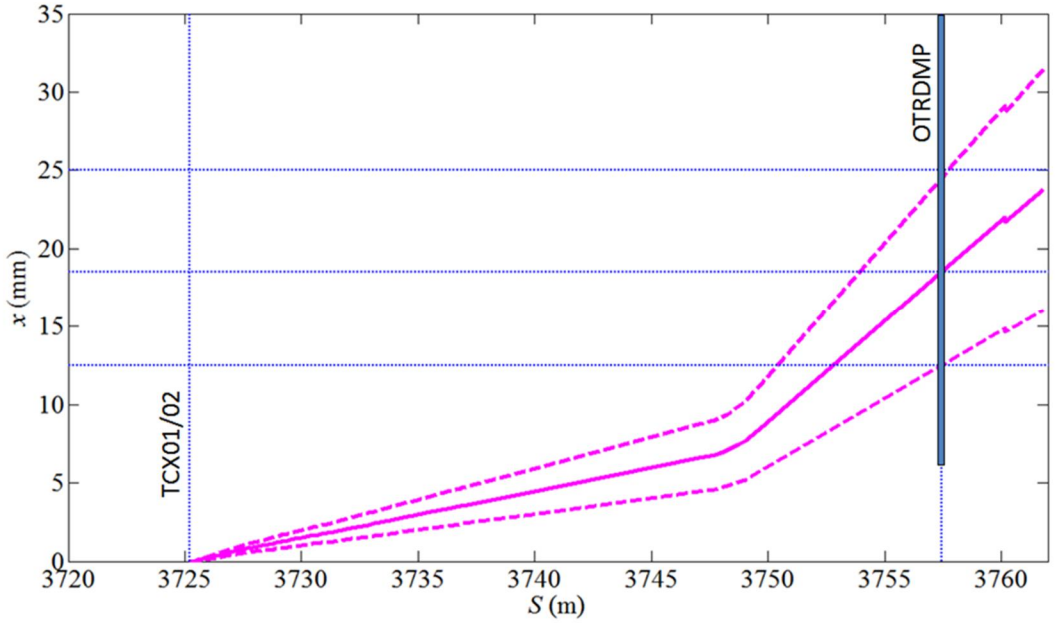

Figure 2: Beam trajectory generated by the XTCAV with a few degrees off the zero-crossing phase. The screen edge is about 6 mm off axis in this drawing (tentative layout) and the center of the kicked beam strikes the screen at x = 18.5 mm. See details in [10].

4. Summary

We discussed a possible layout of the XTCAV system for LCLS-II, and estimated the resolution for both beamlines. With the upgrade of the SLED operation mode, the available power would be enhanced by a factor of 4, which provides the feasibility for the two beamlines sharing one klystron without degrading much the time resolution. The major missing parts in this proposed layout include developing a high-power splitter with flexible power control, fabricating two 1-m long deflecting structures, and some waveguide modifications. We will know better about the SLED operation performance soon in the fall of 2015.

5. Appendix: Two RF components for the LCLS-II deflector system

Appendix-A: High Power Splitter:

The proposed high power splitter is the most compact and simple one-piece X-Band power splitter by Igor Syratchev et al. [8] (CERN). Now this type of power splitter is under fabrication

process and will be installed in the CLIC test stands. The maximum electrical field at 100MW is 50 MV/m, which can be safely used in the LCLS-II deflector system.

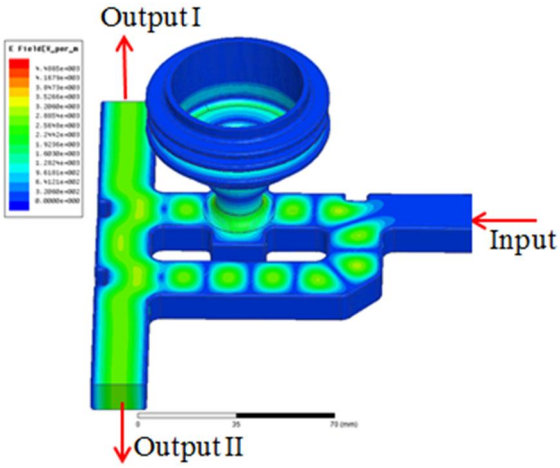

Electrical design simulation

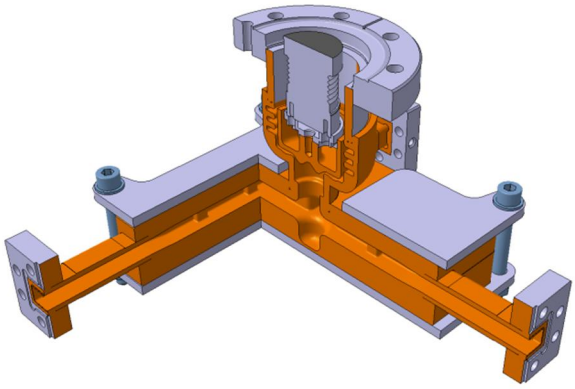

Mechanical design model

Appendix-B: High Power Phase Shifter

The following figure shows the assembly of two deflectors for LCLS I line. The high power phase shifter (circled in red) with 90° phase adjustment range will be removed and used for the LCLS II SXR line. Then, the correct phasing of two deflectors for LCLS I can be obtained by slightly moving the structure positions or slightly deformation of WR90 waveguide.

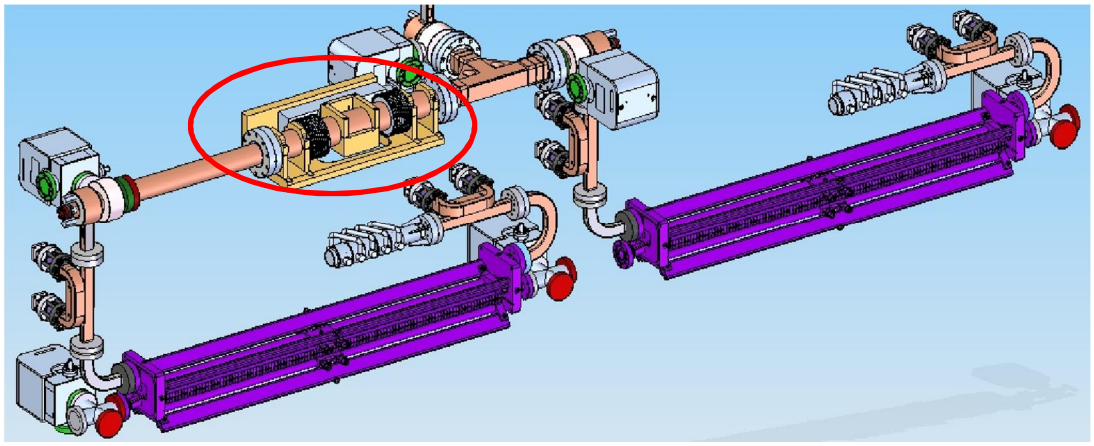

6. References

[1] P. Emma, J. Frisch, & P. Krejcik, A transverse rf deflecting structure for bunch length and phase space diagnostics. SLAC LCLS technical Report LCLS-TN-00-12 (2000).

[2] G. A. Loew and O. H. Altenmueller, Design and applications of RF deflecting structures at SLAC, SLAC-PUB-135 (1965).

[3] V. Dolgashev et al., Design and application of multimegawatt X-band deflectors for femtosecond electron beam diagnostics. Phys. Rev. ST Accel. Beams 17, 102801 (2014).

[4] P. Emma, An X-band transverse rf deflector for the LCLS, SLAC LCLS Technical Note (October 18, 2006).

[5] Y. Ding et al. Femtosecond X-ray pulse temporal characterization in free-electron lasers using a transverse deflector. Phys. Rev. ST Accel. Beams 14, 120701 (2011).

[6] C. Behrens et al., Few-femtosecond time-resolved measurements of X-ray free-electron lasers, Nature Communications, 5, 3762 (2014).

[7] J. Wang, S. Tantawi and C. Xu, Super-compact SLED system used in the LCLS diagnostic system, LINAC14 conference, Geneva, 2014.

[8] The power splitter will use a design from CLIC with some scaling. See this IPAC15 paper https://jacowfs.jlab.org/conf/y15/ipac15/prepress/WEPHA025.PDF.

[9] Z. Li, XTCAV coupler design.

[10] P. Emma, LCLS-II Stay clear requirement PRD.